scientific reports

Check for updates

OPEN

1 ppm-detectable hydrogen gas sensor based on nanostructured polyaniline

Perizat Askar[1], Dana Kanzhigitova[1,2], Aigerim Ospanova[1], Aslan Tapkharov[4], Sagydat Duisenbekov[1], Munziya Abutalip[2], Baktiyar Soltabayev[3], Amanzhol Turlybekuly[3], Salimgerey Adilov[4]✉ & Nurxat Nuraje[1,2]✉

The hydrogen (H_2) energy industry has continued to expand in recent years due to the decarbonization of the global energy system and the drive towards sustainable development. Due to hydrogen's high flammability and significant safety risks, the efficient detection of hydrogen has become an increasingly hot issue today. In this work, a new type of relatively fast and responsive conducting polymer sensor has been demonstrated for tracing H_2 gas in a nitrogen environment. Inspiration of unique properties of carbon nanotube (CNT) and graphene, polyaniline (PANI) hollow nanotubes, PANI thin films are fabricated to study for structural-properties investigation. The PANI hollow nanotube sensor ensures the 1 ppm hydrogen gas detection at room temperature, and exhibits high sensitivity (29%) and fast response and recovery times of 15 and 17 s, follows by PANI thin film sensor (20%), response and recovery times of 65s and 45s. This conducting polymer-based hydrogen sensor holds promise for the early detection of H_2 leaks in a wide range of industries.

As a green energy source, hydrogen is one of the most important potential energy carriers on the way to a more sustainable planet[1]. However, it is a highly flammable, colorless and odorless gas that can cause fire and explosion if not handled properly. Its leakage potentially leads to the explosion as exposed to a flame or static electricity if the volume range exceeds 4% in air[2–4]. Therefore, the minimization of the potential risk by hydrogen needs to be taken into consideration. Furthermore, prompt detection of hydrogen leakage can avoid huge economic loss or the risk of disaster.

To improve the hydrogen sensitivity including detection limits and responsiveness, different types of hydrogen sensors have been developed[5]. These hydrogen gas sensors can be employed across various hydrogen-related industries, including hydrogen fueling stations for vehicles, hydrogen energy facilities, and refineries, to facilitate the early detection of H_2leakages. Among them, the sensors made of organic semiconductor materials with normal temperature operation, solution processability, and flexibility have demonstrated advantages over the inorganic semiconductor based sensors since the inorganic semiconductor-based sensors usually operate at high temperatures and their production is not cost effective[6–10].

Among organic semiconductor materials, conducting polymers (CPs) have actively been investigated for the hydrogen sensor application due to their capability of conducting electricity[11]. Furthermore, the CPs consisting of different levels of conductivity are suitable for reversible doping and dedoping, facilitating them to be repeatedly charged and discharged without losing their electrical conductivity. Since PANI can produce a strong sensor response to alkaline ammonia, a lot of research work has been carried out to study low-concentration sensitive ammonia sensors based on PANI[12,13]. However, the development of hydrogen energy has triggered the exploration of PANI-based hydrogen sensors. Until now, a great deal of research has been conducted on the improvement of CP based sensor's hydrogen detecting capability. These studies have confirmed the important relationship between hydrogen sensitivity and conductivity of the conducting polymers, indicating that hydrogen sensitivity is to a large degree determined by the carrier mobility in the CP[14].

Although various research strategies have been developed for the improvement of the hydrogen sensitivity including detection limit, recovery time and responsiveness, the most promising one is the design of the efficient heterostructured conducting polymer sensor. For example, Bafandeh[15] and his team have improved the H_2 gas sensitivity to 0.4 vol% with 100 s of response time by designing MWCNT/PANI hydrogen gas sensing composite

[1]Department of Chemical and Materials Engineering, School of Engineering & Digital Science, Nazarbayev University, 010000 Astana, Kazakhstan. [2]Lab of Renewable Energy, National Laboratory Astana, Nazarbayev University, 010000 Astana, Kazakhstan. [3]Lab of Advanced Sensors, National Laboratory Astana, Nazarbayev University, 010000 Astana, Kazakhstan. [4]Department of Chemistry, School of Sciences and Humanities, Nazarbayev University, 010000 Astana, Kazakhstan. ✉email: sadilov@nu.edu.kz; nurxat.nuraje@nu.edu.kz

materials. Another heterostructured polypyrrole conducting polymer-based sensor with TiO_2demonstrated the capability of detection of 2500 ppm hydrogen gas with better electron transport[16]. Our recent work based on the heterostructured sensor made of vanadium oxide and polypyrrole(PPY) showed a significant improvement with the detection of 5 ppm hydrogen. In this work, the assembly of vanadium oxide and polypyrrole chains leads to better alignment of polypyrrole chains and enhanced carrier mobility on the PPY chains[17].

These works indicated that the carrier mobility in the CP chains is crucial to hydrogen sensitivity. Despite CP-based gas sensors being inexpensive and simple to manufacture, their sensing performance largely depends on the addition of metals or other carbon materials like CNT and graphene, which increases production costs and complexities. Thus, for the first time we designed the intrinsic conducting polymer sensors inspired by the unique morphologies that can provide better charge transfer and electron mobility such as hollow tube(titania tube, carbon nanotube) and 2D-materials(graphene, TMS, MXene) without applying the strategy of designing heterostructured sensors. For example, hollow titania tubes offered excellent photocatalytic efficiency by high electron mobility and charge transfer due to their directionality relative to other morphologies[18–20]. Graphene and TMS belong to 2D-nanomaterials which can offer high carrier mobility[21–23]. Moreover, carrier mobility in single-walled carbon nanotubes (SWCNTs) is as high as around 10,000 $cm^2\ V^{-1}\ s^{-1}$, whereas the mobility of graphene can reach 15,000 $cm^2\ V^{-1}s^{-1}$[24].

Therefore, based on our strategy that unique morphologies such as nanotubular and 2D- CP nanomaterials offer better carrier mobility and larger charge carriers amount, to obtain better hydrogen sensing performance, three different types of polyaniline nanostructures (such as hollow nanotubes, nanofibers and thin film) were studied in parallel (Fig. 1) and their hydrogen sensing performance has been investigated correlatively with their electrical properties. The findings from this study are expected to bring a light to structure-properties relationship for a highly sensitive hydrogen-based sensor.

Results and discussion

While there is a considerable amount of research on polyaniline's application in detecting toxic gases such as ammonia, carbon monoxide, etc, few studies have been performed on the hydrogen gas sensing mechanism. Recent studies indicated that the heterostructure design of polyaniline composite materials is an important strategy to enhance gas sensing performance through increasing the carrier mobility. However, the fundamental understanding of intrinsic polyaniline hydrogen sensor mechanism has not been fully understood. Thus, based on the hypothesis that the increase of charge carrier concentration and hole mobility through designing hollow tubular and 2D nanostructures of polyaniline lead to high gas sensing performance, we fabricated hollow tubular and film nanostructures of polyaniline inspired by tubular structure (like CNT) and 2D-nanomaterials (like graphene) and tested obtained materials for the hydrogen sensing performance in parallel with short nanofibers via studying the hole mobility and carrier concentration. In this study, the PANI' hollow tubular (Fig. 1a), short nanofiber (Fig. 1b), and thin film (Fig. 1c) were produced by different synthesis methods in combination with interfacial chemical oxidative polymerization. For example, hollow PANI nanotubes (Fig. 1a) were produced by dissolving the PAN core-fiber in the PAN@PANI (core@shell) fibers which were fabricated by interfacial polymerization of aniline monomer at the interface of pre-synthesized polyacrylonitrile (PAN) nanofibers as a template in the presence of ammonium persulfate (APS) oxidants.

Figure S1 shows SEM images of PAN, PANI/PAN nanotubes, and hollow PANI nanotubes at various magnifications. The PAN fibers exhibited a uniform structure with an average diameter of 280 nm, while the PANI/PAN nanofibers have a seamless core/shell structure with a rough surface and an average diameter of 680 nm. Figure S1d verifies total elimination of the PAN core, showing PANI nanotubes with an average thickness of 96 nm. Figure 1b indicates the surface morphologies of the PANI nanofibers synthesized from bicontinouous microemulsion method[25,26]. The PANI nanofibers exhibited short fibers structure with an average diameter of 130 nm (Figure S2d). The PANI thin films (Fig. 1c) were synthesized from ice template approach[27]. In this instance, the single layer of PANI thin film obtained from the ice surface has thickness of approximately 230 nm, as shown in (Figure S2).

The electrical properties of the three different PANI nanomaterials were further investigated via Four-probe and Hall measurement instruments to find the correlation between the PANI's morphologies and their electrical properties toward explaining hydrogen sensing mechanism. Table 1 shows the electrical results including conductivity, hole mobility, and carrier concentration for the three different morphologies of PANI materials. The PANI hollow nanotubes show the best electrical conductivity which is 9.15 S/cm, followed by PANI thin

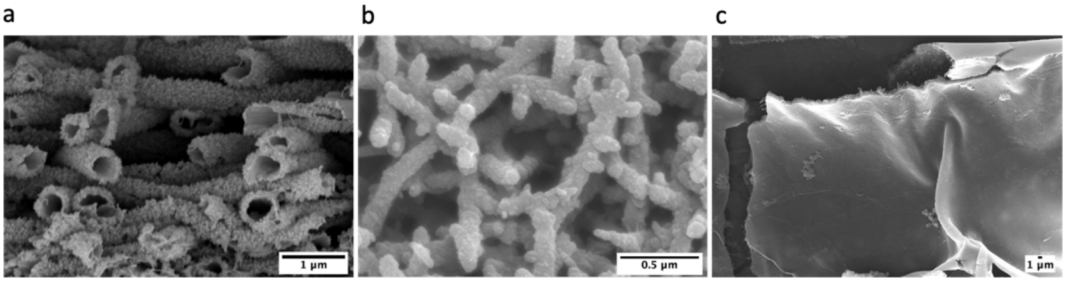

Fig. 1. SEM images of different nanostructured PANI: (**a**) PANI hollow nanotubes, (**b**) PANI nanofibers and (**c**) PANI thin film.

Materials	Electrical conductivity (S/cm)	Mobility (cm^2/Vs)	Standard deviation	Carrier concentration
PANI hollow nanotubes	9.15	100.57	13.06	2.68×10^{17}
PANI thin films	0.6	38.9	1.65	5.01×10^{16}
PANI nanofibers	0.05	4.72	1.05	3.45×10^{16}

Table 1. Electrical properties of fabricated PANI materials.

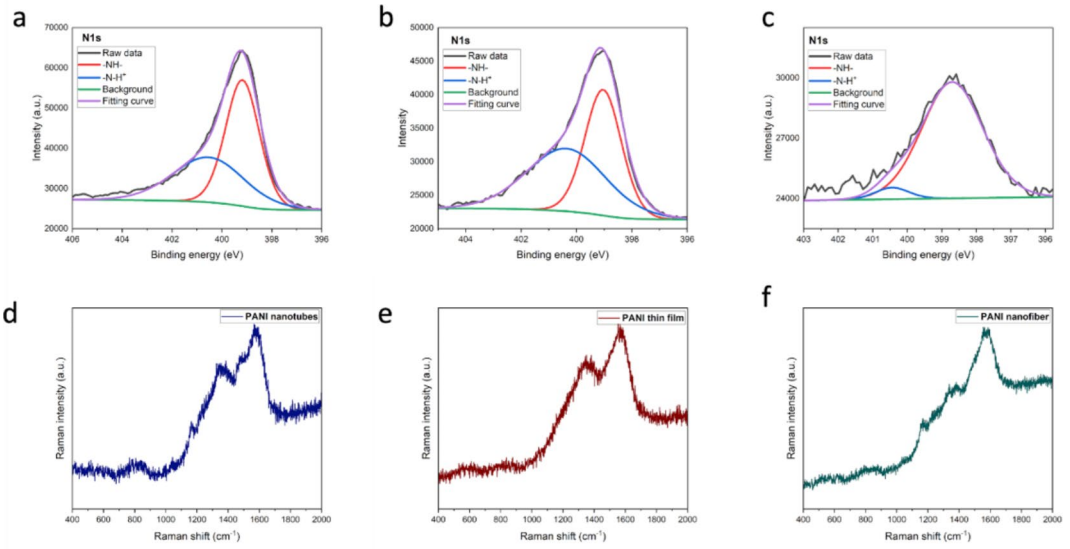

Fig. 2. The results of X-ray photoelectron spectroscopy (XPS) spectra and Raman spectra analysis: (**a**) XPS of PANI hollow nanotubes, (**b**) XPS of PANI thin film, (**c**) XPS of PANI nanofibers, (**d**) Raman spectra of PANI hollow nanotubes, (**e**) Raman spectra of PANI ice film, (**f**) Raman spectra of PANI nanofibers.

film (0.60 S/cm), then PANI nanofibers (0.05 S/cm) via Four-probe measurement. The mobility and carrier concentration data were measured from the Hall effect measurement system.

The electrical conductivity is proportional to both carrier concentration and hole mobility as shown in Eq. 1.

$$\sigma = \mathrm{ne}\mu, \tag{1}$$

where is electrical conductivity. and represent carrier concentration and mobility.

The PANI hollow nanotube likewise possessed the highest carrier mobility, 100.57 cm^2/Vs. It shows at least 2 times higher than the PANI thin film, and 5 times higher than nanofibers. Furthermore, the carrier concentrations for both PANI nanotubes (Table 1) was found to be a ten times as high (around 10^{17} $/cm^3$) as that of and PANI thin film and nanofibers ($10^{16}/cm^3$). This variation can be attributed to the alignment of the conducting polymer, which facilitates the formation of pathways for carrier transfer, thereby enhancing electrical characteristics such as carrier mobility and conductivity.

These findings were consistent with the electrical conductivity of PANI nanomaterials and indicated the important correlation between carrier transport/concentration and morphology is crucial to explain hydrogen sensing performance[28].There are great examples that can be found in the effect of certain morphologies on the overall device performance. For example, Poly(3-hexylthiophene) (P3HT) thin films containing nanowire morphologies exhibit a high value of 0.02 $cm^2\ V^{-1}\ s^{-1}$, which is almost ten times greater than the mobilities of P3HT thin films lacking any specific form[29,30]. Also, the PEDOT nanotubes as counter electrodes for DSSCs showed 8.3% of remarkable power conversion efficiency (PCE), setting a new record which can be attributed to the increased effective area of the oriented PEDOT nanotubes[31].

To further confirm the high carrier concentrations for the PANI film and nanotube found by Hall measurement, both X-ray photoelectron spectroscopy (XPS) and Raman spectroscopy techniques were further performed to analyze the polaron concentration for all of the samples, indicating the carrier concentrations in the PANI nanomaterials. The polaron information can be found at the N1s core peak in the XPS spectra (Fig. 2a–c) respectively for the hollow nanotubes, thin film, and nanofibers of PANI. At binding energies greater than 400 eV, positively charged nitrogen species can be found. These species correspond to a specific oxidation level and/or the degree of protonation[32–34]. The peak observed at 400.4 eV is associated with nitrogen atoms that have delocalized radical cations, also known as polarons. The N1s of PANI tend to be deconvoluted into two peaks around, the -NH- at 400 eV and the =N-H+ at 402 eV[35,36]. The =N-H+ polaron charge carrier species can be found in the N1s core level for the PANI hollow nanotube, PANI thin film, and PANI nanofiber at around

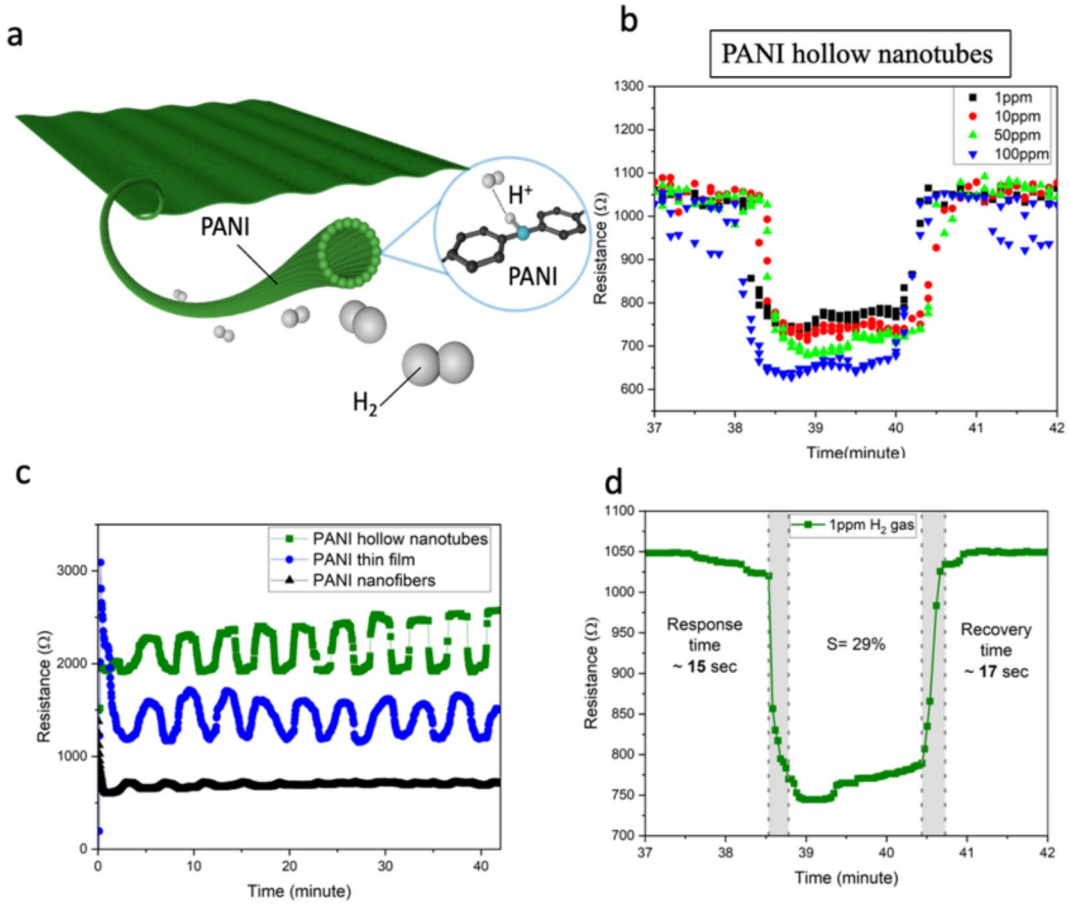

Fig. 3. (**a**) Schematic illustration for interaction of H_2 molecules with PANI hollow nanotube; (**b**) H_2 concentration depends response of PANI hollow nanotubes sensor; (**c**) comparison of responses in different PANI at 1 ppm H_2 detection; (**d**) response time of hollow PANI nanotubes sensor at 1 ppm H_2 gas.

399.18, 399.08 and 398.68 eV. Further doping increases the intensity and area of the =N-H+ peak, indicating a high doping degree in a higher conductivity value.

Therefore, we propose that the PANI hollow structure, containing a higher concentration of polaron species, showed significantly increased electrical conductivity, leading to enhanced sensitivity towards hydrogen gas. In contrast, the PANI nanofibers had the lowest level of bipolaron species, which indicated insufficient doping and the least favorable reaction to hydrogen gas, accompanied by low conductivity. The PANI nanofibers exhibited a significant rise in the strength of the quinone-diimine peaks (Fig. 2c). Ice-assisted approach produced highly conducting PANI nanosheets that facilitated effective charge transport due to polaron delocalization and enhanced backbone ordering[37]. Conversely, there was a substantial drop in the intensity of the peaks corresponding to semiquinone cationic radicals. Overall, the hollow nanotube structure could offer a structured channel for charge carriers in one dimension. This could enhance the efficiency of charge transport and minimize charge carrier recombination, resulting in an increased charge carrier density and, consequently, a higher concentration of polarons.

Raman spectra for PANI nanotubes, thin films, and nanofibers are displayed in (Fig. 2d–f). Their spectra were analyzed individually in three distinct ranges that correspond to different vibration modes. These modes included the bending modes of the C-H bonds between 1100 and 1210 cm^{-1}, the stretching modes of the C-C bonds between 1520 and 1650 cm^{-1}, and the various stretching modes of the C-N bonds (polarons) between 1210 and 1520 $cm^{[-1}$[38,39]. The C-N bands observed in PANI nanotubes and PANI thin film have a larger and sharper shape compared to the C-N bands observed in PANI nanofiber. The changes were ascribed to the arrangement of quinoid and benzenoid units due to the template-assisted approaches. Another distinct band observed for the spectra of PANI nanotubes and PANI thin films between 1350 and 1375 cm^{-1} was relatively decreased and shifted to 1384 cm^{-1} for the PANI nanofibers.

Our hypothesis was further testified via the hydrogen sensing measurement using three different PANI nanomaterials in a nitrogen atmosphere in correlation with their electric properties. Sensitivity refers to the changes in resistance of a sensing film relative to its initial resistance when exposed to a gas. Response is determined by a mathematical equation:

$$\text{Response} = (R_0 - R_{gas})/R_0 * 100\%, \quad (2)$$

where R_0 is the electrical resistance of the sensor material in a nitrogen gas environment, and R_{gas} is the electrical resistance values of the sensor upon exposure to H_2 gas, respectively.

The high conductivity leads to a low initial resistance, denoted as R_0, and a high relative sensitivity, expressed as $\Delta R/R_0$[40,41]. This is because the initial resistance is in the denominator of the relative response equation[42]. The gas sensor's response time was determined as the interval from the onset of target gas exposure to reaching 90% of the response, while recovery time was measured as the duration from the cessation of gas exposure until the sensor returned to background levels[43].

Although the three PANI nanomaterials demonstrated different responses for hydrogen gas (Fig. 3c), the PANI hollow nanotubes provided accurate hydrogen detection at low concentrations (1 ppm) with a fast response and recovery time, and also had better sensitivity among them. Figure 3b indicated the response of the PANI hollow nanotubes sensor versus time for various concentrations of H_2 in the range of 1-100 ppm. The response of the PANI hollow nanotubes sensor increased as the concentration of H_2 gas increased. The response and recovery curve of the PANI hollow nanotubes sensor at 1ppm H_2 gas is demonstrated in Fig. 3d, which shows response/recovery times were 15s and 17s. The PANI hollow nanotubes can react with hydrogen within a few seconds, and allows hydrogen atoms to diffuse into the pores and interact with the nanotube's surface molecules. The high mobility and high carrier concentrations in PANI hollow nanotubes allows more free charge carriers to participate in the sensing reaction, resulting in improved detection sensitivity even at low hydrogen concentrations (1-ppm) shown in (Fig. 3b). The second highest response sensor is the PANI thin film, followed by PANI nanofiber which can barely show response at 1ppm H_2 gas. Since the PANI thin films can offer relatively better connections among polymer chains than PANI nanofibers, they demonstrate efficient responses in conductivity when exposed to hydrogen. Comparing to PANI hollow nanotubes (29%) PANI thin film shows less sensitivity (20%) and slower response/recovery times 65 and 45s (Figure S5) since the PANI thin film possess relatively less hole mobility and carrier concentration. Table 2 compares different CP hydrogen sensors in the literature and our work, PANI hollow nanotubes show very short response time and high sensitivity for 1 ppm hydrogen detection.

PANI is a p-type semiconductor material and holes behave as the main carriers. This possible hydrogen detection mechanism is that hydrogen dissociates and binds to the nitrogens along the polyaniline chain, and this interaction increases the number of charge carriers (i.e., holes), and reduces the resistance of PANI[46]. The polyaniline undergoes subsequent charge transfer between neighboring amine nitrogens, causing it to switch back to its polaronic, doped, emeraldine salt state. This reversible interaction process ultimately leads to a change in conductivity. It is generally accepted that the sensing mechanism can be explained by the adsorption-desorption of target gas molecules on the surface of the sensor, which causes a change in conductivity and affects the doping levels[47,48]. The doping level, which determines the redox reaction, can be altered by the transfer of electrons to or from the target gas, resulting in a change in resistance.

As discussed above, our sensing results demonstrate that the presence of H_2 gas molecules leads to a decrease in the material's resistance (Fig. S6). Figure 3a shows the hydrogen sensing mechanism of PANI hollow nanotubes sensors, where hydrogen molecules dissociates and binds to the polyaniline chain, then lead to increase of the number of charge carriers. The high mobility in PANI hollow nanotubes allows more free charge carriers to participate in the sensing reaction, resulting in improved detection sensitivity even at low hydrogen concentrations shown in (Fig. 3b). The PANI hollow nanotubes, which have organized and confined pathways, enhance the interaction between hydrogen molecules and charge carriers. This interaction enhances the movement of electric charge, enabling a very effective and rapid reaction to gas molecules[49]. The enhanced electrical conductivity of nanotubes, as compared to the other structures PANI, can be attributed to their orderly arrangement within the nanotube architecture. PANI nanotubes possess a one-dimensional tubular structure, creating a well-defined channel for the movement of charge carriers in improving charge carrier mobility and reducing the chances of scattering charges. However, the usage of the ice template technique successfully achieved regulated morphology, which can be attributed to the observed enhancement in the electrical conductivity of the PANI thin film compared to PANI nanofibers. Producing a layer on an ice surface leads to a highly organized and aligned structure, enhancing the arrangement of polymer chains and facilitating the flow of electric charge, which provides better conductivity.

To explore the potential real-world application of pure aniline as a hydrogen sensing material, we selected PANI hollow nanotubes (which demonstrated the highest sensitivity) to test their selectivity for three different gas mixtures, including hydrogen, as well as to assess the effect of humidity and environmental conditions on sensing stability. Figure S7 illustrates the selectivity of the fabricated PANI nanotube sensor, highlighting its significantly higher sensitivity to hydrogen compared to other gases, such as methane and carbon dioxide. While

Sensing materials	H_2 gas concentration	Sensitivity	Response time	References
polyaniline/TiO_2	2500 ppm	9.05	94s	Kafash et al., 2022[16]
PANI/Sm_2O_3	10,000 to 80,000 ppm	3.94	7s	Jamnani et al., 2020[50]
MWNT/PANI	500 ppm	2.1	150s	Shrivastava et al., 2023[51]
MWCNTs/PANI	0.4 vol%	25	100s	Bafandeh et al., 2023[15]
PANI hollow nanotubes	1 to 100 ppm	29	15s	This work
PANI thin film	1 to 100 ppm	20	65s	This work
PANI nanofiber	1 to 100 ppm	6	102s	This work

Table 2. Comparison of different CP based hydrogen gas sensors.

the sensor displayed strong selectivity for hydrogen over carbon-based gases, challenges related to humidity and environmental effects on PANI-based sensors, as reported in previous studies[44,45], were confirmed in our experiments. From Figure S8, it can be seen that the resistance of the PANI hollow nanotube sensor under varying humidity levels (0%, 25%, 50%, 75%) demonstrates a clear trend where the baseline resistance decreases with increasing humidity. In dry conditions, the sensor's resistance is highest, while at higher humidity levels, the resistance gradually decreases. This shift in resistance aligns with the known behavior of PANI, where water molecules can influence the polymer's protonation state, thereby reducing its resistance. Despite these changes in resistance, the sensor maintains its sensitivity to hydrogen across all humidity levels, as seen in the consistent responsiveness of the sensor in the figure. The fluctuations in resistance at each humidity level demonstrate that the sensor continues to detect hydrogen effectively, although the baseline resistance is affected by moisture in the environment. Figure S9shows the stability of fabricated in air condition, the interaction of PANI with various gases (included water vapor) can cause changes in its chemical structure. The presence of moisture can mask the sensor's response to hydrogen gas, leading to false readings or diminished sensitivity[44,45].

Conclusion

In this study, three different PANI sensors consisting of hollow tube, film and short nanofiber were evaluated for hydrogen sensing. Among them, the PANI hollow nanotubes exhibited excellent detection performance compared to the thin film sensors, and obtained a response of 29% in the experimental data, with a response time of 15 s, which has better performance than PANI thin film (20%). PANI nanofiber sensor did not show the visiable response at 1ppm hydrogen gas. The sensing performance of the hollow tubes were directly proportional to their carrier mobility and carrier concentration. In addition, the hollow nanotube structure polyaniline provided the best conductivity (9.15 S/cm), followed by PANI thin film (0.60 S/cm) and PANI nanofiber (0.05 S/cm). Compared with the polyaniline thin film and short nanofibers, the obtained hollow nanotubes polyaniline has a tubular structure similar to carbon nanotubes, which provides a better connection network to conduct electrons better. This finding gives some insight into structure-property studies of polyaniline nanostructures and H_2 gas sensing mechanism.

Methods

Materials

All solvents and chemicals were of analytical grade and used without further purification, which include Ammonium peroxydisulfate (APS) (98.0%, Sigma-Aldrich), hydrochloric acid(HCl) (37%, Sigma Aldrich), cyclohexane (99.9%, Sigma-Aldrich), sodium dodecyl sulfate (SDS)(99.0% ,Sigma-Aldrich), 1-Pentanol (99.9%, Sigma-Aldrich), polyacrylonitrile (PAN) (Sigma-Aldrich, Mw = 150,000), acetone (99.5%, Sigma-Aldrich), ethanol (EtOH), conductive silver paint(PELCO®). Aniline (99.5%, Sigma–Aldrich) was distilled under reduced pressure before use.

Preparation of PAN fibers

Polyacrylonitrile (PAN) nanofibers were used as a temporary template in the fabrication process of PANI hollow nanotubes. A 10.0 mL syringe equipped with a needle diameter of 0.9 mm containing 10 w.t.% solution of PAN in N, N-dimethylformamide (DMF) was used to fabricate electrospun nanofibers, where the syringe was then connected to a syringe pump for controlling flow rate of the polymer solution at 1.2 ml/h. The distance from needle to plane collector was 17 cm. A positive voltage of 15 kV was applied during the electrospinning process at ambient conditions.

Preparation of hollow PANI nanotubes

The fabrication method for hollow PANI nanotubes was adapted from the literature report[52,53]. The PAN template nanofibers were first soaked in 25 ml of a 0.2 M aniline solution in 1 M HCl for 2 h at 4 °C. Following that, a 25 ml of solution containing 0.2 M APS in 1 M HCl was slowly poured into the reaction vessel to initiate the polymerization reaction of PANI on the PAN template. Following 24-hours, the nanofibers were immersed in DMF for another 24 h in order to selectively dissolve the PAN core from the core-shell structure that were produced, while the hollow PANI nanotubes remains unaffected. After that, the hollow nanotubes were put into a vacuum oven set at a temperature of 45 °C for a duration of 5 h to eliminate any residual solvent.

Synthesis of polyaniline ice films

Figure S3a illustrates the synthesis procedure of PANI thin film by the method described in Ref[27].. An inverted surface of ice from the Petri dish was applied to form smooth PANI film before putting the aniline solution in 1 M HCl over the smooth cooled ice. Right after the aniline solution spread uniformly, the APS in 1 M HCl solution was dropped onto the top of the ice to keep the reaction temperature at 8 °C. Protonated aniline may be successfully adsorbed by OH groups on the ice surface via hydrogen bonding and electrostatic interactions. PANI-ICE formation was evident to the naked eye after 3 min of oxidative polymerization.

Synthesis of polyaniline particles

Polyaniline nanofibers were synthesized via the bicontinuous microemulsion(BM) polymerization method (Fig. S3b) described in literature[25]. In this experiment, APS dissolved in deionized water was combined with a SDS/pentanol (mass ratio of 2:3) surfactant solution, and mixed with cyclohexane/monomer(6:1 w.t.) solution. The system formed a bicontinuous phase and began polymerization to obtain a uniformly structure conducting polymer[26,54]. After 24 h at room temperature, the green powders of PANI are formed and should be washed with acetone to remove all unreacted impurities and monomers.

Data availability

The data that support the findings of this study are available within the article (and its Supplementary Information files) and from the corresponding authors upon reasonable request.

Received: 5 April 2024; Accepted: 18 October 2024
Published online: 06 November 2024

References

1. Panarello, D. & Gatto, A. Decarbonising Europe – EU citizens' perception of renewable energy transition amidst the European Green Deal. *Energy Policy* **172**, 113272 (2023).
2. Najjar, Y. S. Hydrogen leakage sensing and control: (review). *Biomed. J. Sci. Tech. Res.* **21** 16228–16240 (2019).
3. Koo, W. T. et al. Chemiresistive hydrogen sensors: fundamentals, recent advances, and challenges. *ACS Nano* **14**, 14284–14322 (2020).
4. Buttner, W. J., Post, M. B., Burgess, R. & Rivkin, C. An overview of hydrogen safety sensors and requirements. *Int. J. Hydrogen Energy* **36**, 2462–2470 (2011).
5. Li, J. et al. Local dynamic neural network for quantitative analysis of mixed gases. *Sens. Actuators B Chem.* **404**, 135230 (2024).
6. Li, Y. et al. Pd-Decorated ZnO Hexagonal Microdiscs for NH_3 Sensor. *Chemosensors* 12, (2024).
7. Yoon, H. Current trends in sensors based on conducting polymer nanomaterials. *Nanomaterials* **3**, 524–549 (2013).
8. Chen, Y. et al. Room-Temperature optoelectronic NO_2 sensing using two-Dimensional Gallium oxyselenides. *ACS Appl. Nano Mater.* **7**, 3229–3238 (2024).
9. Khaniyev, B. et al. The Improved Non-Polar Gas Sensing Performance of Surface-Modified Porous Silicon-Based Gas Sensors. *Coatings* 13, (2023).
10. Khaniyev, B. A., Sagidolda, Y., Dikhanbayev, K. K., Tileu, A. O. & Ibraimov, M. K. High sensitive NH_3 sensor based on electrochemically etched porous silicon. *Cogent Eng.* **7**, (2020).
11. Al-Mashat, L., Tran, H. D., Wlodarski, W., Kaner, R. B. & Kalantar-Zadeh, K. Conductometric hydrogen gas sensor based on polypyrrole nanofibers. *IEEE Sens. J.* **8**, 365–369 (2008).
12. Duan, X. et al. Enhanced NH3 sensing performance of polyaniline via a facile morphology modification strategy. *Sens. Actuators B Chem.* **369**, 132302 (2022).
13. Liu, C. et al. Local gaussian process regression with small sample data for temperature and humidity compensation of polyaniline-cerium dioxide NH_3 sensor. *Sens. Actuators B Chem.* **378**, 133113 (2023).
14. Alberti, G., Zanoni, C., Losi, V., Magnaghi, L. R. & Biesuz, R. Current trends in polymer based sensors. *Chemosensors* **9**, (2021).
15. Bafandeh, N. et al. Carbon nanotubes/polyaniline as hydrogen gas sensor: optical bandgap, micro-morphology, and skin depth studies. *AIP Adv.* **13**, (2023).
16. Kafash, S. & Milani Moghaddam, H. Porous polyaniline tube-like/TiO_2 nano-heterostructure for sensing hydrogen gas at environmental conditions. *Int. J. Hydrogen Energy* **47**, 14740–14758 (2022).
17. Kanzhigitova, D. et al. p-Toluenesulfonic acid doped vanadium pentoxide/polypyrrole film for highly sensitive hydrogen sensor. *Adv. Compos. Hybrid. Mater.* **6**, 218 (2023).
18. Hou, H. et al. Efficient photocatalytic activities of TiO_2 hollow fibers with mixed phases and mesoporous walls. *Sci. Rep.* **5**, 1–9 (2015).
19. Absalan, Y. et al. Titania nanotubes (TNTs) prepared through the complex compound of gallic acid with titanium; examining photocatalytic degradation of the obtained TNTs. *Arab. J. Chem.* **13**, 7274–7288 (2020).
20. Pratibha, Kapoor, A. & Rajput, J. K. Nanostructured materials for the visible-light driven hydrogen evolution by water splitting: a review. *Int. J. Hydrogen Energy* **47**, 17544–17582 (2022).
21. Shiraz, H. G., Crispin, X. & Berggren, M. Transition metal sulfides for electrochemical hydrogen evolution. *Int. J. Hydrogen Energy* **46**, 24060–24077 (2021).
22. Zhang, C. et al. Two-dimensional transition metal carbides and nitrides (MXenes): synthesis, properties, and electrochemical energy storage applications. *Energy Environ. Mater.* **3**, 29–55 (2020).
23. Gosling, J. H. et al. Universal mobility characteristics of graphene originating from charge scattering by ionised impurities. *Commun. Phys.* **4**, (2021).
24. Sun, X., Sun, H., Li, H. & Peng, H. Developing polymer composite materials: Carbon nanotubes or graphene? *Adv. Mater.* **25**, 5153–5176 (2013).
25. ZHU Yan, C. H. E. N., Shao-Jie, T. I. A. N., Long-Zhao, Y. U. A. N. & Shuai, Y. A. O. W. Q. Phase diagram and temperature influence of SDS/n-pentanol-cyclohexane-water pseudo ternary systems. *Chem. J. Chin. Universities* **34**, 1254–1257 (2013).
26. Abutalip, M. et al. Strategic synthesis of 2D and 3D conducting polymers and derived nanocomposites. *Adv. Mater.* **2208864**, 1–8 (2022).
27. Choi, I. Y. et al. High-conductivity two-Dimensional Polyaniline Nanosheets developed on ice surfaces. *Angew. Chem. Int. Ed.* **54**, 10497–10501 (2015).
28. Prins, P. et al. High intrachain hole mobility on molecular wires of ladder-type poly(p-phenylenes. *Phys. Rev. Lett.* **96**, 1–4 (2006).
29. Tran, H. D., Li, D. & Kaner, R. B. One-dimensional conducting polymer nanostructures: bulk synthesis and applications. *Adv. Mater.* **21**, 1487–1499 (2009).
30. Merlo, J. A. & Frisbie, C. D. Field effect transport and trapping in regioregular polythiophene nanofibers. *J. Phys. Chem. B* **108**, 19169–19179 (2004).
31. Yin, Z. & Zheng, Q. Controlled synthesis and energy applications of one-dimensional conducting polymer nanostructures: an overview. *Adv. Energy Mater.* **2**, 179–218 (2012).
32. Kohut-Svelko, N. et al. Study of a nanocomposite based on a conducting polymer: Polyaniline. *Langmuir* 21, 1575–1583 (2005).
33. Zeng, X. R. & Ko, T. M. Structures and properties of chemically reduced polyanilines. *Polym. (Guildf)* **39**, 1187–1195 (1998).
34. Karatchevtseva, I., Zhang, Z., Hanna, J. & Luca, V. Electrosynthesis of macroporous polyaniline - V_2O_5 nanocomposites and their unusual magnetic properties. *Chem. Mater.* **18**, 4908–4916 (2006).
35. Han, M. G. & Im, S. S. X-ray photoelectron spectroscopy study of electrically conducting polyaniline/polyimide blends. *Polym. (Guildf)* **41**, 3253–3262 (2000).
36. Zeng, X. & Ko, T. Structure—Conductivity relationships of Iodine-doped. 1993–2001 (1997).
37. Kim, K., Kim, B., Kim, K. & Park, M. J. Ten-minute synthesis of highly conductive polymer nanosheets on ice surfaces: role of ice crystallinity. *Macromol. Rapid Commun.* **42**, 1–8 (2021).
38. Snežzana Miljanić, L. & Frkanec Tomislav Biljan, 3 Zlatko Meić Mladen Žini ć. Recent advances in linear and nonlinear Raman spectroscopy I. *J. Raman Spectrosc.* **38**, 1538–1553 (2007).
39. Bernard, M. C. & Hugot-Le Goff, A. Snežzana Miljanić, Leo Frkanec, Tomislav Biljan, 3 Zlatko Meić Mladen Žinić. Quantitative characterization of polyaniline films using Raman spectroscopy. II. Effects of self-doping in sulfonated polyaniline. *Electrochim. Acta* **38**, 1538–1553 (2007).
40. Turlybekuly, A. et al. Sensitivity enhancement of CO_2 sensors at Room Temperature based on the CZO Nanorod Architecture. *ACS Sens.* **21**, 16228–16240 (2011).

41. Rakhmanova, A. et al. Application of response surface methodology for optimization of nanosized zinc oxide synthesis conditions by electrospinning technique. *Nanomaterials* **12**, (2022).
42. Brie, M., Turcu, R., Neamtu, C. & Pruneanu, S. The effect of initial conductivity and doping anions on gas sensitivity of conducting polypyrrole films to NH_3. *Sens. Actuators B Chem.* **37**, 119–122 (1996).
43. Turlybekuly, A., Sarsembina, M., Mentbayeva, A., Bakenov, Z. & Soltabayev, B. CuO/TiO_2 heterostructure-based sensors for conductometric NO_2 and N_2O gas detection at room temperature. *Sens. Actuators B Chem.* **397**, 134635 (2023).
44. Sharma, H. J., Sonwane, N. D. & Kondawar, S. B. Electrospun SnO_2/Polyaniline composite nanofibers based low temperature hydrogen gas sensor. *Fibers Polym.* **16**, 1527–1532 (2015).
45. Abuzalat, O., Wong, D., Park, S. S. & Kim, S. High-Performance, Room Temperature Hydrogen Sensing with a Cu-BTC/Polyaniline Nanocomposite Film on a Quartz Crystal Microbalance. *IEEE Sens. J.* **19**, 4789–4795 (2019).
46. Virji, S., Kaner, R. B. & Weiller, B. H. Hydrogen sensors based on conductivity changes in polyaniline nanofibers. *J. Phys. Chem. B* **110**, 22266–22270 (2006).
47. Husain, A. & Shariq, M. U. Polypyrrole nanocomposites as promising gas/vapour sensing materials: past, present and future prospects. *Sens. Actuators Phys.* **359**, (2023).
48. Sen, T., Mishra, S. & Shimpi, N. G. Synthesis and sensing applications of polyaniline nanocomposites: a review. *RSC Adv.* **6**, 42196–42222 (2016).
49. Chen, X., Shen, L., Yuan, C. A., Wong, C. K. Y. & Zhang, G. Molecular model for the charge carrier density dependence of conductivity of polyaniline as chemical sensing materials. *Sens. Actuators B Chem.* **177**, 856–861 (2013).
50. Jamnani, S. R., Moghaddam, H. M., Leonardi, S. G. & Neri, G. PANI/Sm_2O_3 nanocomposite sensor for fast hydrogen detection at room temperature. *Synth. Met.* **268**, 116493 (2020).
51. Shrivastava, S. et al. Effect of MWNT concentration on hydrogen gas sensing property of MWNT-ployaniline composite. *Int. J. Hydrogen Energy* **48**, 38107–38117 (2023).
52. Haghighat Bayan, M. A., Afshar Taromi, F., Lanzi, M. & Pierini, F. Enhanced efficiency in hollow core electrospun nanofiber-based organic solar cells. *Sci. Rep.* **11**, 1–11 (2021).
53. Miao, Y. E., Fan, W., Chen, D. & Liu, T. High-performance supercapacitors based on hollow polyaniline nanofibers by electrospinning. *ACS Appl. Mater. Interfaces* **5**, 4423–4428 (2013).
54. Kanzhigitova, D. et al. Controlled synthesis of polyaniline-based nanomaterials with self-assembly and interface manipulation. *Langmuir*https://doi.org/10.1021/acs.langmuir.3c03167 (2023).

Acknowledgements

This work was supported by the Ministry of Education and Science of the Republic of Kazakhstan under project No.AP23487622, "Fabrication of controlled nanostructures of conducting polymers and their composites to improve hydrogen gas sensing"; Faculty-development Competitive Research Grants Program of Nazarbayev University for 2023-2025 (Project ref. no. 20122022FD4114), "Fabrication of Nanostructured Conducting Polymers and Their Nanocomposites for Energy Applications"; Ministry of Education and Science of the Republic of Kazakhstan under project No. BR21882439, "Advancement of the Green Energy: Foundational Research of Solar Fuel Technologies for Sustainable Production and Advanced Storage". Special thanks to Bakyt Khaniyev from the Department of Physics and Technology, Al-Farabi Kazakh National University for conducting ammonia gas sensing test and help us with comments.

Author contributions

N. N. led the team for the research project. S. A., M. A. supervised the project. P. A. designed and performed the experiments for the synthesis of PANI, and the characterization including sensing performance, electrical properties test and the overall analysis. D. K. aided in the characterization and analysis of XPS, Raman and the scientific discussions. A. O. contributed to the electrospinning process and PANI hollow nanotubes synthesis. A. T. and S. T. contributed to SEM characterization and analysis. B.S. and A.T. analyzed all the gas sensing experiments and results. All authors discussed the results and comments on the manuscript. P. A. and N.N. wrote the paper.

Declarations

Competing interests

The authors declare no competing interests.

Additional information

Supplementary Information The online version contains supplementary material available at https://doi.org/10.1038/s41598-024-77083-5.

Correspondence and requests for materials should be addressed to S.A. or N.N.